Electronic Supplementary Information

Invigorating the Catalytic Performance of CoP through Interfacial Engineering by Ni_2P Precipitation

Junyu Zhang,[a] Sufeng Wei,[b] Yan Liu,[c] Guoyong Wang,[,a] Yuhuan Cui,[a] Anqi Dong,[a] Shan Xu,[a] Jianshe Lian,[a] Qing Jiang[a]*

[a.] Key Laboratory of Automobile Materials, Department of Materials Science and Engineering, Jilin University, Changchun, 130025, PR China. E-mail: materwanggy@jlu.edu.cn

[b.] Key Laboratory of Advanced Structural Materials, Changchun University of Technology, Changchun, 130012, PR China

[c.] Key Laboratory of Bionic Engineering (Ministry of Education) and State Key Laboratory of Automotive Simulation and Control, Jilin University, Changchun 130022, PR China

KEYWORDS: Catalytic properties, Gibbs free energy, Metal phosphides, Interfacial energy, Surface engineering

- *Corresponding author.
- †Electronic supplementary information (ESI) available.

Experimental details

Preparation of CoP/Ni_2P catalyst. Firstly, 0.75 mmol of $Co(Ac)_2 \cdot 4H_2O$ (99 wt%, Tianjin Guangfu Fine Chemical Research Institute) and 0.75 mmol of $Ni(Ac)_2 \cdot 4H_2O$ (99 wt%, Tianjin Guangfu Fine Chemical Research Institute) were dissolved into 10 ml of 1,3-propanediol (99 wt%, Aladdin) and sonicated at least 30 minutes. Then, 40 ml of isopropanol (99.8 wt%, BeiJing Chemical Works, 99.8%) was added into the solution. After sonication for 10 minutes, the final solution was transferred to a Teflon-lined stainless steel autoclave and heated to 160 ℃ for 12 h. Then cooled down to room temperature. The precursors were collected, washed with ethanol for several times and dried in a vacuum oven at 70 ℃ for 12 h. Finally, the precursors (0.1 g in a porcelain boat) and NaH_2PO_2 (1.0 g in another porcelain boat) were placed at two separate positions of the tube furnace. The samples were heated at 350 ℃ for 2 h with a ramping rate of 3 ℃ min^{-1} in Ar atmosphere, then naturally cooled down to room temperature. The obtained products were thoroughly washed with deionized water to remove any residual salts and then dried in a vacuum oven at 60 °C.

Structural Characterization. Crystal structures of the as-synthesized catalysts were examined by an X-Ray diffraction (XRD) using a Cu Kα radiation source (Rigaku, D/max 2500PC). Scanning electron microscopy (SEM) images were obtained with a field emission scanning electron microscopy (FESEM; JSM-6700F). The Energy dispersive X-ray spectroscopy (EDS) was obtained by Oxford Instruments X-MAX. Transmission electron microscope (TEM) and high-resolution transmission electron microscope (HRTEM) images were obtained using JEM-2100F with an accelerating voltage of 200 kV. X-ray photoelectron spectroscopy (XPS) experiments were performed on an ESCALab MK Ⅱ electron spectrometer (Vacuum Generators) with unmonochromatic 240 W Al Kα X-rays. The propotion of Ni and Co in electrolyte before and after long-term durability test was measured by inductively coupled plasma-atomic emission spectrometry (ICP-OES, ThermoScientific iCAP6300).

Preparation of Working Electrode and Electrochemical Test. 3 mg sample was dispersed in 550 μL of water/ethanol/ 5 wt% Nafion (V / V / V = 250: 250: 50) and sonicated for at least 20 min. Then 4 μL of the

catalyst ink was pipetted onto a glassy carbon electrode (GCE, Φ = 3 mm) with a loading of 0.31 mg/cm^2.

All electrochemical measurements of various catalysts were performed on an electrochemical workstation (CHI 750E) with a three-electrode setup. A glassy carbon electrode coated, a graphite rod and saturated calomel electrode (SCE) were used as working, counter and reference electrode at 0.5 M H_2SO_4 and 1 M PBS electrolyte, and for 1 M KOH electrolyte, the Hg|HgO electrode was used as reference electrode. The electrolyte was bubbled with O_2 and H_2 for 20 min prior to OER and HER measurements. Linear scanning voltammetry (LSV) was carried out at a scan rate of 5 mV s^{-1} in various pH electrolyte at room temperature, and the time-dependent current density curves were recorded under respective overpotential. The electrochemical impedance spectroscopy (EIS) measurements were carried out from 10 kHz to 0.01 Hz with an overpotential of 100 mV. All LSV polarization curves have been iR-corrected. The measured potentials *vs.* SCE reference electrode were converted to the RHE according to the Nernst equation:

$$E_{(RHE)} = E_{(SCE)} + 0.0591 \times pH + 0.241 \text{ (V)}$$

where $E_{(SCE)}$ is the applied potential *vs.* SCE and 0.241 V is the standard potential of the SCE reference electrode at 25 °C, and for Hg|HgO electrode, the standard potential is replaced by 0.098 V.

The overall water splitting was performed in a two-electrode system, one CoP/Ni_2P electrode served as the negative electrode for HER and another CoP/Ni_2P electrode acted as the positive electrode for OER. The catalytic durability of the two-electrode full cell system for overall water splitting was tested in 1.0 M KOH electrolyte at an applied potential to reach an initial catalytic current density of 10 mA cm^{-2}.

In this work, we use electrochemical double layer capacitance (C_{dl}) to characterize the electrochemical active surface area (ECSA). The C_{dl} was measured by cyclic voltammograms in a potential region of 0.1 V to 0.3 V vs RHE with different scan rate of 20 to 140 mV/s. The C_{dl} is estimated by plotting the Δj at 0.2 V vs. RHE against the scan rates, where the slope is twice C_{dl}. The ECSA of 1 cm^2 is represented by a special capacitance value of 0.2 mF/cm^2. ECSA and ECSA current density (j_{ECSA}) were calculated by the following equation:

$$ECSA = C_{dl}\ (mF\ cm^{-2}) / 0.2\ (mF\ cm^{-2})$$

$$j_{ECSA} = I\ (mA) / ECSA\ (cm^2)$$

Cyclic voltammetry measurements of our samples were carried out in PBS electrolyte (PH=7) with a potential window from −0.2 to 0.6 V vs RHE and a scan rate of 50 mV/s. Assuming one electron redox process, the integrated charge over the whole potential range was divided by two. Then, the value was divided by the Faraday constant to get the number of active sites for different samples. The turnover frequency (s^{-1}) can be estimated according to this equation:

$$TOF = jS / 2nF$$

where j is the current density measured, S is the surface area of the electrode, F is the Faraday constant (96485.30 C/mol), n is the number of the active sites (mol) for different samples, and number 2 is 2 electrons per mole of hydrogen.

Figures:

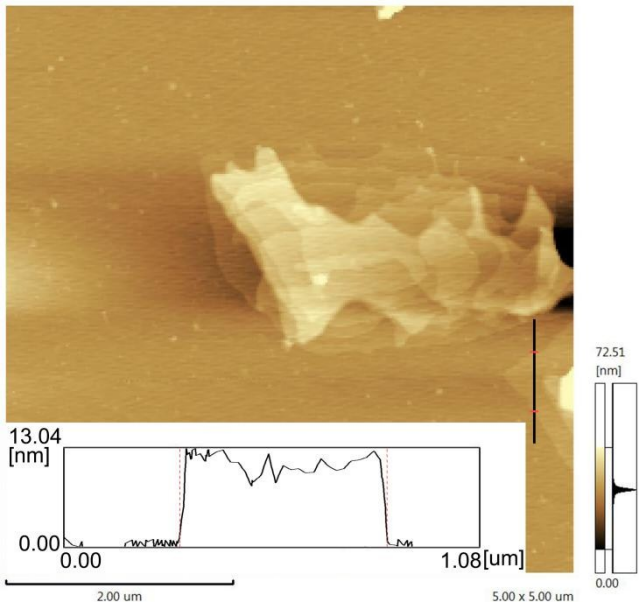

Fig. S1 AFM images of CNOH-2 and corresponding depth analysis.

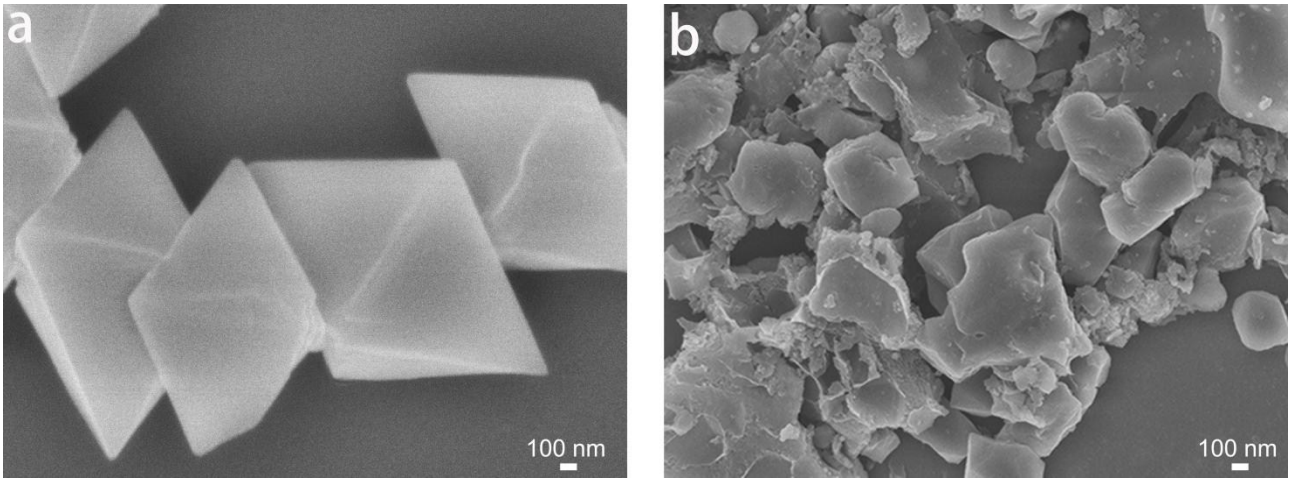

Fig. S2 FESEM images of pure $Ni(OH)_2$ and pure Ni_2P.

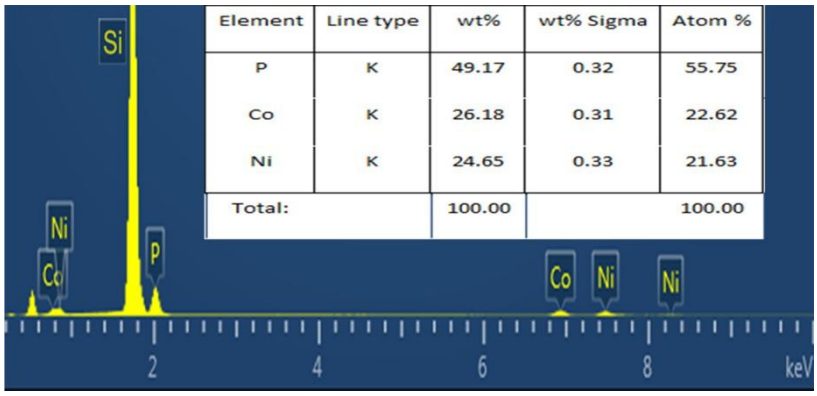

Element	Line type	wt%	wt% Sigma	Atom %
P	K	49.17	0.32	55.75
Co	K	26.18	0.31	22.62
Ni	K	24.65	0.33	21.63
Total:		100.00		100.00

Fig. S3 The energy dispersive X-ray spectrum for the CNP-2 (Ni : Co = 1 : 1) hybrids.

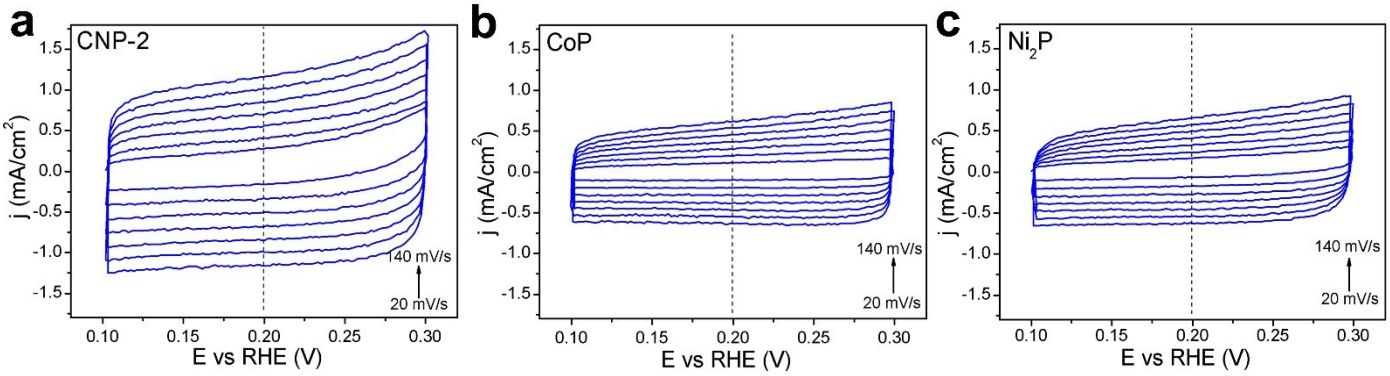

Fig. S4 CV curves of (a) Ni_2P, (b) CoP and (c) CNP-2 with various scan rates (20, 40, 60, 80, 100, 120 and 140 mV s^{-1}). The capacitive current from double layer charging can be measured from CV data in a potential range where no faradaic processes observed.

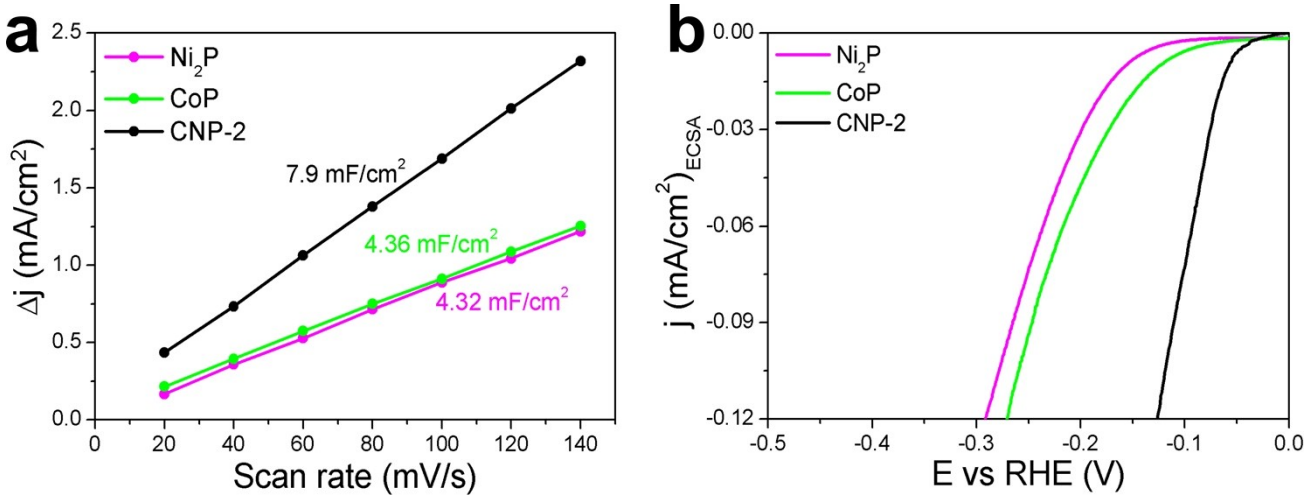

Fig.S5 (a) The C_{dl} for Ni_2P, CoP and CNP-2 at 0.2 V. (b) LSVs of Ni_2P, CoP and CNP-2 normalized to the electrochemically active surface area (ECSA).

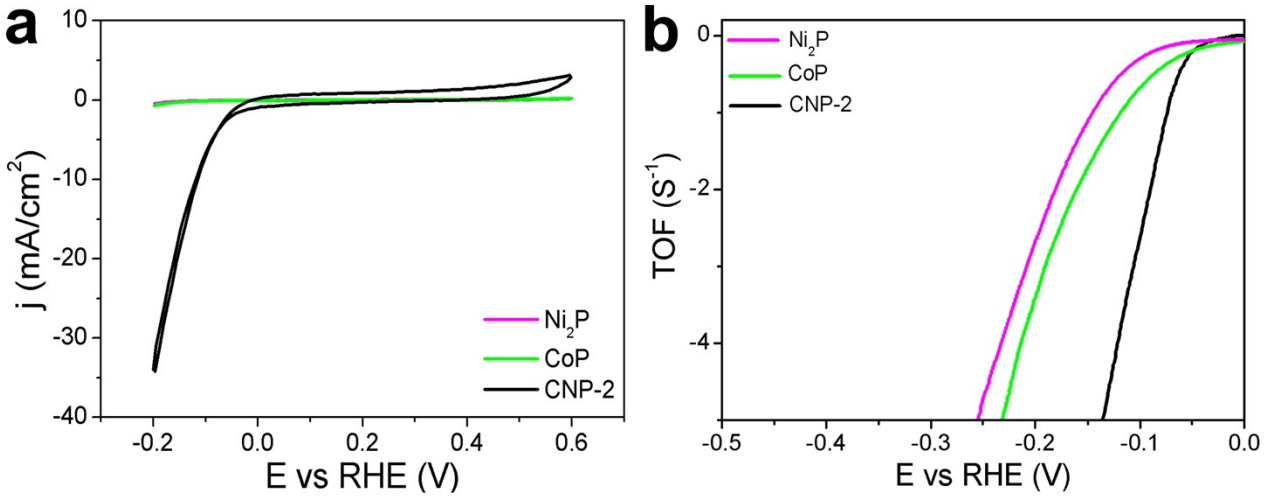

Fig.S6 (a) The cyclic voltammetrys for CNP-2, CoP and Ni_2P catalysts in 1.0 M PBS (pH=7) at a scan rate of 50 mV/s. (b) The corresponding TOF curves for the catalysts in the range of the applied potentials.

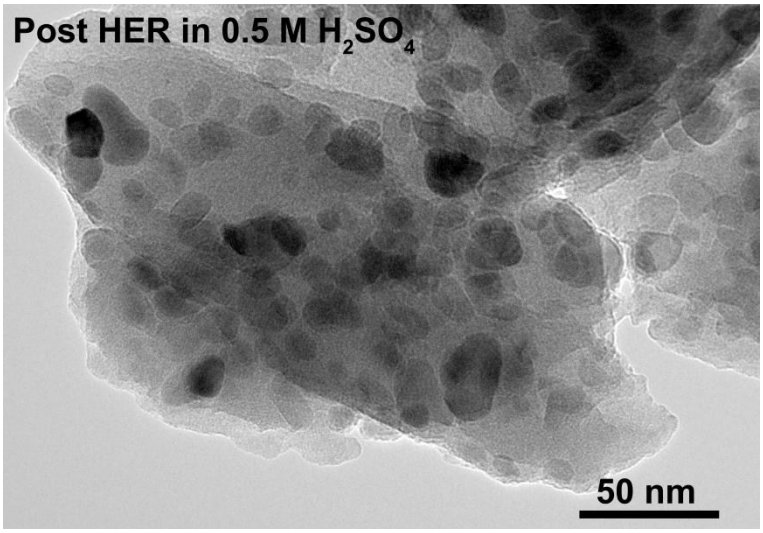

Fig. S7 TEM image of the CNP-2 catalyst after 20 h HER durability testing in 0.5 M H_2SO_4.

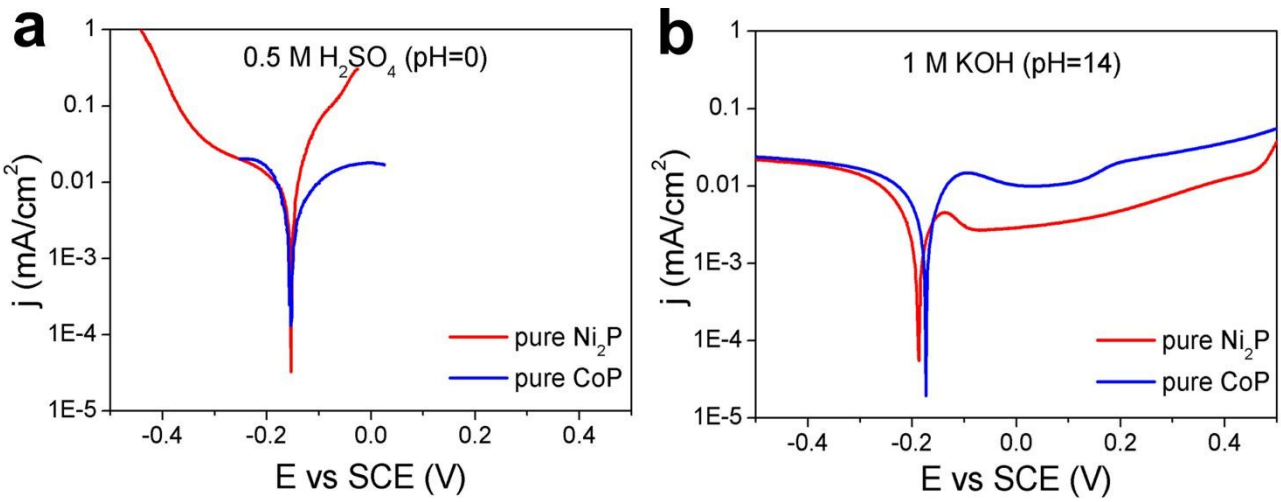

Fig. S8 Potentiodynamic curves of pure Ni_2P and pure CoP at pH=0 and pH=14 environment.

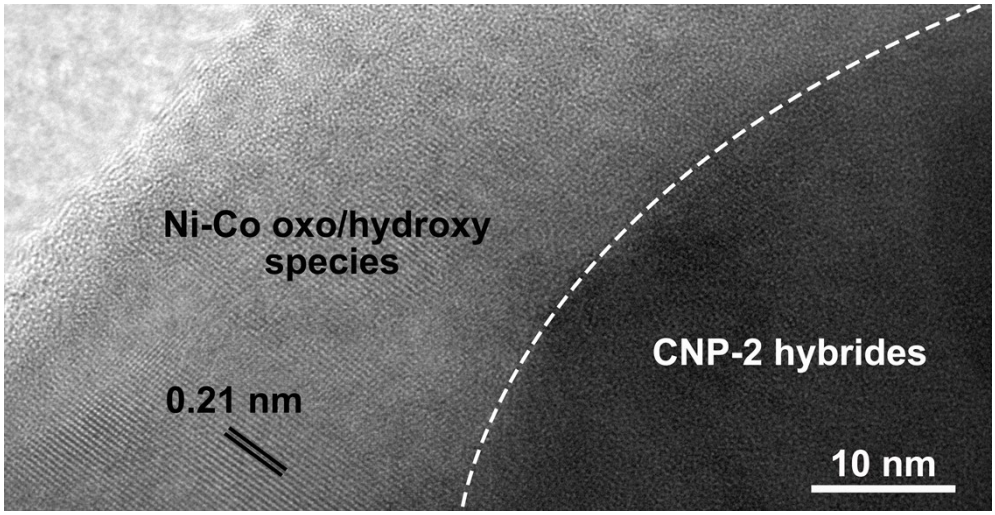

Fig. S9 HRTEM image of the CNP-2 catalyst after OER process in 1.0 M KOH electrolyte.

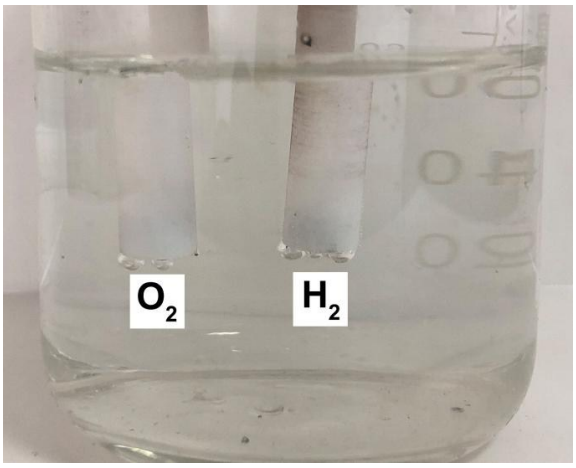

Fig. S10 The photo of the overall water splitting cell.

Table S1 The concentration of Co and Ni before and after potentiostatic test in 0.5 M H_2SO_4.

Element	**Original electrolyte** (ug/mL)	**After test** (ug/mL)
Co	0	0.0742
Ni	0	0.0695

Table S2 Comparison of HER performance in 0.5 M H_2SO_4 for CNP-2 with other HER catalysts.

Catalyst	Overpotential (mV, j=10 mA/cm²)	Tafel slope (mV/dec)	Reference
CNP-2	55	54	This work
Ni_2P/CNT	124	53	[1]
$Ni_{12}P_5$ spheres	144	46	[2]
Ni_5P_4-Ni_2P-NS	130	79	[3]
Ni_5P_4 NC	175	42	[4]
CoP NP	85	50	[5]
CoP NW	100	51	[6]
CoP-CNTs	139	52	[7]
CoP NTs	129	60	[8]
CoP CPHs	133	51	[9]
C@Ni-Co-P	110	48	[10]
Co-Fe-P 3D electrode	80	45	[11]
CoNi/NC	142	105	[12]

Table S3 Comparison of HER performance in 1.0 M PBS buffer for CNP-2 hybrids with other HER catalysts.

Catalyst	Overpotential (mV, j=10 mA/cm²)	Tafel slope (mV/dec)	Reference
CNP-2	133	94	This work
NiP_2/CC	136	103	[13]
CoP-400	161	81	[14]
CoP/PCNF	191	111	[15]
Porus Ni_2P polyhedron	160	78	[16]
Ni_2P/Ni	190	142	[17]
NiP_x-coated CC	230	101	[18]
Co-NRCNTs	540	-	[19]
CoP NA/CC	145	123	[20]

Table S4 Comparison of HER performance in 1.0 M KOH for CNP-2 hybrids with other non-precious HER catalysts.

Catalyst	Overpotential (mV, j=10 mA/cm^2)	Tafel slope (mV/dec)	Reference
CNP-2	200	112	This work
CoP NW	209	129	6
CoP/CC	209	129	6
Co-NRCNTs	370	-	19
Ni_2P	220	-	21
NiCoP/rGO	270	124	22
Co@N-C	210	108	23
Ni/NiS	230	115	24
CoO_x@CN	232	82	25

Table S5 Comparison of OER performance in 1.0 M KOH for CNP-2 hybrids with other representative catalysts

Catalyst	Overpotential (mV, j=10 mA/cm^2)	Tafel slope (mV/dec)	Reference
CNP-2	300	62	This work
Co-P film	345	47	26
NiCoP microspheres	340	86	27
NiCoP NPs	310	52	27
CoP/rGO hybrids	340	66	28
Ni-P	300	64	29
Fe-Ni oxide	375	-	30
NiFe-NS	302	67	31
Ni-Co binary oxides	325	45	32
NiCo LDH	367	66	33

Table S6 The concentration of Co and Ni before and after EWS test in 1.0 M KOH.

Element	Original electrolyte (ug/mL)	After test (ug/mL)
Co	0	0.0563
Ni	0	0.0527

References:

1. Y. Pan, W. Hu, D. Liu, Y. Liu and C. Liu, *J. Mater. Chem. A*, 2015, **3**, 13087-13094.
2. J. Chang, S. Li, G. Li, J. Ge, C. Liu and W. Xing, *J. Mater. Chem. A*, 2016, **4**, 9755-9759.
3. X. Wang, Y. V. Kolen'ko, X. Q. Bao, K. Kovnir and L. Liu, *Angew. Chem. Int. Ed. Engl.*, 2015, **54**, 8188-8192.
4. Y. Pan, Y. Liu, J. Zhao, K. Yang, J. Liang, D. Liu, W. Hu, D. Liu, Y. Liu and C. Liu, *J. Mater. Chem. A*, 2015, **3**, 1656-1665.
5. E. J. Popczun, C. G. Read, C. W. Roske, N. S. Lewis and R. E. Schaak, *Angew. Chem. Int. Ed. Engl.*, 2014, **53**, 5427-5430.
6. J. Tian, Q. Liu, A. M. Asiri and X. Sun, *J. Am. Chem. Soc.*, 2014, **136**, 7587-7590.
7. C. Wu, Y. Yang, D. Dong, Y. Zhang and J. Li, *Small*, 2017, **13**.
8. H. Du, Q. Liu, N. Cheng, A. M. Asiri, X. Sun and C. M. Li, *J. Mater. Chem. A*, 2014, **2**, 14812-14816.
9. M. Xu, L. Han, Y. Han, Y. Yu, J. Zhai and S. Dong, *J. Mater. Chem. A*, 2015, **3**, 21471-21477.
10. Y. Bai, H. Zhang, L. Liu, H. Xu and Y. Wang, *Chem.*, 2016, **22**, 1021-1029.
11. Y. Tan, H. Wang, P. Liu, Y. Shen, C. Cheng, A. Hirata, T. Fujita, Z. Tang and M. Chen, *Energy Environ. Sci.*, 2016, **9**, 2257-2261.
12. J. Deng, P. Ren, D. Deng and X. Bao, *Angew. Chem. Int. Ed. Engl.*, 2015, **54**, 2100-2104.
13. X. Wang, H. Zhou, D. Zhang, M. Pi, J. Feng and S. Chen, *J. Power Sources*, 2018, **387**, 1-8.
14. H. Li, X. Zhao, H. Liu, S. Chen, X. Yang, C. Lv, H. Zhang, X. She and D. Yang, *Small*, 2018, **14**, e1802824.
15. H. Lu, W. Fan, Y. Huang and T. Liu, *Nano Res.*, 2018, **11**, 1274-1284.
16. L. Yan, P. Dai, Y. Wang, X. Gu, L. Li, L. Cao and X. Zhao, *ACS Appl. Mater. Int.*, 2017, **9**, 11642-11650.
17. Y. Shi, Y. Xu, S. Zhuo, J. Zhang and B. Zhang, *ACS Appl. Mater. Int.,* 2015, **7**, 2376-2384.
18. M. Chen, J. Qi, W. Zhang and R. Cao, *Chem. Commun.*, 2017, **53**, 5507-5510.
19. X. Zou, X. Huang, A. Goswami, R. Silva, B. R. Sathe, E. Mikmekova and T. Asefa, *Angew. Chem. Int. Ed. Engl.*, 2014, **53**, 4372-4376.
20. T. Liu, L. Xie, J. Yang, R. Kong, G. Du, A. M. Asiri, X. Sun and L. Chen, *ChemElectroChem*, 2017, **4**, 1840-1845.
21. L. A. Stern, L. Feng, F. Song and X. Hu, *Energy Environ. Sci.*, 2015, **8**, 2347-2351.
22. J. Li, M. Yan, X. Zhou, Z. Huang, Z. Xia, C. Chang, Y. Ma and Y. Qu, *Adv. Funct. Mater.*, 2016, **26**, 6785-6796.
23. J. Wang, D. Gao, G. Wang, S. Miao, H. Wu, J. Li and X. Bao, *J. Mater. Chem. A*, 2014, **2**, 20067-20074.
24. G. Chen, T. Y. Ma, Z. Liu, N. Li, Y. Su, K. Davey and S. Qiao, *Adv. Funct. Mater.*, 2016, **26**, 3314-3323.
25. H. Jin, J. Wang, D. Su, Z. Wei, Z. Pang and Y. Wang, *J. Am. Chem. Soc.*, 2015, **137**, 2688-2694.
26. N. Jiang, B. You, M. Sheng and Y. Sun, *Angew. Chem. Int. Ed. Engl.*, 2015, **54**, 6251-6254.

27. C. Wang, J. Jiang, T. Ding, G. Chen, W. Xu and Q. Yang, *Adv. Funct. Mater.*, 2016, **3**, 1500454.
28. L. Jiao, Y. Zhou and H. Jiang, *Chem. Sci.*, 2016, **7**, 1690-1695.
29. X. Yu, Y. Feng, B. Guan, X. (David) Lou and U. Paik, *Energy Environ. Sci.*, 2016, **9**, 1246-1250.
30. J. Landon, E. Demeter, N. İnoğlu, C. Keturakis, I. E. Wachs, R. Vasić, A. I. Frenkel and J. R. Kitchin, *ACS Catal.*, 2012, **2**, 1793-1801.
31. F. Song and X. Hu, *Nat. Commun.*, 2014, **5**, 4477.
32. Y. Yang, H. Fei, G. Ruan, C. Xiang and J. M. Tour, *ACS Nano*, 2014, **8**, 9518-9523.
33. H. Liang, F. Meng, M. Caban-Acevedo, L. Li, A. Forticaux, L. Xiu, Z. Wang and S. Jin, *Nano Lett.*, 2015, **15**, 1421-1427.